A Correlation between Lipid Domain Shape and Binary Phospholipid Mixture Composition in Free Standing Bilayers: A Two-Photon Fluorescence Microscopy Study

Luis A. Bagatolli and Enrico Gratton
Laboratory for Fluorescence Dynamics, University of Illinois at Urbana-Champaign, Urbana, Illinois 61801-3080 USA

ABSTRACT Giant unilamellar vesicles (GUVs) composed of different phospholipid binary mixtures were studied at different temperatures, by a method combining the sectioning capability of the two-photon excitation fluorescence microscope and the partition and spectral properties of 6-dodecanoyl-2-dimethylamino-naphthalene (Laurdan) and Lissamine rhodamine B 1,2-dihexadecanoyl-*sn*-glycero-3-phosphoethanolamine (*N*-Rh-DPPE). We analyzed and compared fluorescence images of GUVs composed of 1,2-dilauroyl-*sn*-glycero-3-phosphocholine/1,2-dipalmitoyl-*sn*-glycero-3-phosphocholine (DLPC/DPPC), 1,2-dilauroyl-*sn*-glycero-3-phosphocholine/1,2-distearoyl-*sn*-glycero-3-phosphocholine (DLPC/DSPC), 1,2-dilauroyl-*sn*-glycero-3-phosphocholine/1,2-diarachidoyl-*sn*-glycero-3-phosphocholine (DLPC/DAPC), 1,2-dimyristoyl-*sn*-glycero-3-phosphocholine/1,2-distearoyl-*sn*-glycero-3-phosphocholine (DMPC/DSPC) (1:1 mol/mol in all cases), and 1,2-dimyristoyl-*sn*-glycero-3-phosphoethanolamine/1,2-dimyristoyl-*sn*-glycero-3-phosphocholine (DMPE/DMPC) (7:3 mol/mol) at temperatures corresponding to the fluid phase and the fluid-solid phase coexistence. In addition, we studied the solid-solid temperature regime for the DMPC/DSPC and DMPE/DMPC mixtures. From the Laurdan intensity images the generalized polarization function (GP) was calculated at different temperatures to characterize the phase state of the lipid domains. We found a homogeneous fluorescence distribution in the GUV images at temperatures corresponding to the fluid region for all of the lipid mixtures. At temperatures corresponding to phase coexistence we observed concurrent fluid and solid domains in the GUVs independent of the lipid mixture. In all cases the lipid solid domains expanded and migrated around the vesicle surface as we decreased the temperature. The migration of the solid domains decreased dramatically at temperatures close to the solid-fluid→solid phase transition. For the DLPC-containing mixtures, the solid domains showed line, quasicircular, and dendritic shapes as the difference in the hydrophobic chain length between the components of the binary mixture increases. In addition, for the saturated PC-containing mixtures, we found a linear relationship between the GP values for the fluid and solid domains and the difference between the hydrophobic chain length of the binary mixture components. Specifically, at the phase coexistence temperature region the difference in the GP values, associated with the fluid and solid domains, increases as the difference in the chain length of the binary mixture component increases. This last finding suggests that in the solid-phase domains, the local concentration of the low melting temperature phospholipid component increases as the hydrophobic mismatch decreases. At the phase coexistence temperature regime and based on the Laurdan GP data, we observe that when the hydrophobic mismatch is 8 (DLPC/DAPC), the concentration of the low melting temperature phospholipid component in the solid domains is negligible. This last observation extends to the saturated PE/PC mixtures at the phase coexistence temperature range. For the DMPC/DSPC we found that the nonfluorescent solid regions gradually disappear in the solid temperature regime of the phase diagram, suggesting lipid miscibility. This last result is in contrast with that found for DMPE/DMPC mixtures, where the solid domains remain on the GUV surface at temperatures corresponding to that of the solid region. In all cases the solid domains span the inner and outer leaflets of the membrane, suggesting a strong coupling between the inner and outer monolayers of the lipid membrane. This last finding extends previous observations of GUVs composed of DPPE/DPPC and DLPC/DPPC mixtures (Bagatolli and Gratton, 2000, *Biophys. J.* 78:290–305).

INTRODUCTION

Over the past 30 years studies of lipid-lipid and lipid-protein interactions in model systems were carried out on small and large unilamellar vesicles (SUVs and LUVs, respectively) as well as multilamellar vesicles (MLVs). These lipid structures, which are characterized by high curvature radius and an average diameter of hundreds of nanometers, are too small to be good models for cell membranes. Instead, giant unilamellar vesicles (GUVs) have diameters between 5 and 200 μm. These "cell size" vesicles are becoming objects of intense scrutiny in diverse areas that focus on membrane behavior (Menger and Keiper, 1998). Many studies of membrane physics have used GUVs, particularly studies of the mechanical properties of model membranes (Evans and Kwok, 1982; Needham et al., 1988; Needham and Evans, 1988; Meléard et al., 1997, 1998; for reviews see Sackmann, 1994, and Menger and Keiper, 1998). These studies revealed the physical properties of the membranes through

Received for publication 27 January 2000 and in final form 15 March 2000.

Address reprint requests to Dr. Enrico Gratton, Laboratory for Fluorescence Dynamics, 184 Loomis Lab., 1110 West Green, Urbana, IL 61801. Tel.: 217-244-5620; Fax: 217-244-7187; E-mail: enrico@scs.uiuc.edu.

Dr. Bagatolli's present address is Instituto de Investigaciones Bioquimicas de Bahia Blanca (UNS/CONICET), CC857, B8000 FWB, Bahia Blanca, Buenos Aires, Argentina. Tel: +54-291-4861201; Fax: +54-291-4861200; E-mail: lbagatol@criba.edu.ar.

0006-3495/00/07/434/14 $2.00

the calculation of elementary deformation parameters. In recent years, studies of lipid-protein and lipid-DNA interactions were also performed using GUVs (Wick et al., 1996; Longo et al., 1998; Angelova et al., 1999; Holopainen et al., 2000). A very interesting approach consists of injecting or adding femtoliter amounts of DNA or protein solutions to GUVs with a microinjector and then following morphological changes in single vesicles by conventional microscope techniques (phase contrast or fluorescence; Wick et al., 1996; Angelova et al., 1999; Holopainen et al., 2000). As Menger and Keiper mentioned in their review article, GUVs are being examined by multiple disciplines with multiple approaches and objectives (Menger and Keiper, 1998). Still, the use of GUVs in biophysics is in an early stage of development.

The phase equilibria in lipid mixtures were extensively studied in the last 25 years. The phase diagrams for different lipid mixtures have been constructed using both theoretical and experimental approaches, particularly for binary phospholipid mixtures. Theoretical calculations were made with computer models to build the phospholipid phase diagrams (Ipsen and Mouritsen, 1988; Jørgensen and Mouritsen, 1995). Also, an array of experimental techniques such as differential scanning calorimetry, fluorescence spectroscopy, NMR, x-ray diffraction, and electron spin resonance have been used to construct lipid phase diagrams of binary mixtures, mainly using MLVs, SUVs, or LUVs (Lee, 1975; Lentz et al., 1976; Mabrey and Sturtevant, 1976; Van Dijck et al., 1977; Arnold et al., 1981; Blume et al., 1982; Caffrey and Hing, 1987; Shimshick and McConnell, 1973). The most attractive region in lipid phase diagrams of binary mixtures is that corresponding to the coexistence of the fluid and solid phases. In recent years, lipid domains in vesicles at the phase coexistence region were visualized directly with electron microscopy techniques (see, for example, Sackmann, 1978). However, as was pointed by Raudino, no direct and detailed knowledge of domain shapes in vesicles was available (Raudino, 1995). Actually, there is a dearth of experimental approaches that allow the direct visualization of lipid domains (shape and dynamics) in lipid vesicles, using the same experimental conditions as classical approaches (such as, for example, differential scanning calorimetry and fluorescence spectroscopy).

GUVs are a very attractive system in which to study phase equilibria of pure lipid systems and lipid mixtures with microscopy techniques, mainly because single vesicles can be observed under the microscope. However, there are few studies using GUVs to directly observe lipid phase equilibria. Haverstick and Glaser were the first to visualize lipid domains in GUVs with fluorescence microscopy and digital image processing (Haverstick and Glaser, 1987). These authors directly visualized Ca^{2+}-induced lipid domains in erythrocyte ghosts, GUVs formed of mixtures of phosphatidylcholine (PC) phospholipid and acidic phospholipids, and GUVs formed of natural lipids from the erythrocyte membrane at constant temperature. They showed that the size and distribution of the Ca^{2+}-induced domains depend on phospholipid composition (Haverstick and Glaser, 1987). In addition, Glaser and co-workers also studied the lipid domain formation caused by the addition of proteins and peptides in GUV membranes (Haverstick and Glaser, 1989; Glaser, 1992; Yang and Glaser, 1995).

The direct visualization of the microscopic scenario of lipid phase equilibria by two-photon excitation fluorescence microscopy was recently reported for single GUVs composed of pure components and binary lipid mixtures (Bagatolli et al., 1999; Bagatolli and Gratton, 1999, 2000). For example, in the case of single phospholipid component GUVs, we reported that during the heating cycle the GUV shows a polygonal shape only at the phase transition temperature region (Bagatolli and Gratton, 1999). The proposed microscopic picture of the GUV polygonal shape was explained by considering that the gel-phase regions of the lipid bilayer become planar and that the vesicle bends along fluid line defects formed by liquid crystalline domains (Bagatolli and Gratton, 1999). For phospholipid binary mixtures we showed fluorescence images obtained with three different probes at temperatures corresponding to the fluid phase and at the phase coexistence region for 1,2-dimiristoyl-*sn*-glycero-3-phosphoethanolamine/1,2-dipalmitoyl-*sn*-glycero-3-phosphocholine (DPPE/DPPC) and 1,2-dilauroyl-*sn*-glycero-3-phosphocholine/1,2-dipalmitoyl-*sn*-glycero-3-phosphocholine (DLPC/DPPC) mixtures (Bagatolli and Gratton, 2000). At the phase coexistence temperature regime different shapes of micron-sized solid domains, depending on the binary mixture composition, were observed. These solid-phase lipid domains expanded and migrated around the vesicle surface as we decreased the temperature (Bagatolli and Gratton, 2000). Furthermore, for the DPPE/DPPC mixture, separated domains that remain in the GUV surface were observed at the solid temperature regime, showing solid-solid lipid immiscibility. From the 6-dodecanoyl-2-dimethylamino-naphthalene (Laurdan) intensity images, the excitation generalized polarization (GP) function was calculated to characterize the phase state of the lipid domain (Bagatolli et al., 1999; Bagatolli and Gratton, 2000). In all cases the domains span the inner and outer leaflets of the bilayer, suggesting a strong coupling between the inner and outer monolayers of the lipid membrane (Bagatolli et al., 1999; Bagatolli and Gratton, 2000). This observation is in agreement with that reported in the work of Korlach et al., in which the lipid domain in mixtures of DLPC/DPPC/POPS and DLPC/DPPC/POPS/cholesterol is directly visualized at room temperature by confocal microscopy (Korlach et al., 1999). These authors also measured the diffusion coefficient of fluorescent probes in the region of phase coexistence, using fluorescence correlation spectroscopy (FCS).

Our approach, based on the sectioning effect of the two-photon fluorescence microscope and the well-characterized fluorescent properties of 6-dodecanoyl-2-dimethylamine-naphthalene (Laurdan) and Lissamine rhodamine B 1,2-

dihexadecanoyl-*sn*-glycero-3-phosphoethanolamine (*N*-Rh-DPPE), allowed us to study the relationship between domain shape and lipid composition in saturated PC-containing binary mixtures. We also investigated and compared the solid temperature regime in GUVs composed of 1,2-dimyristoyl-*sn*-glycero-3-phosphoethanolamine/1,2-dimyristoyl-*sn*-glycero-3-phosphocholine (DMPE/DMPC) and 1,2-dimyristoyl-*sn*-glycero-3-phosphocholine/1,2-distearoyl-*sn*-glycero-3-phosphocholine (DMPC/DSPC). We show novel microscopic pictures of lipid lateral organization in single vesicles at the different temperature regimes. The unique properties of unsupported GUVs allows us to make new observations of the shape and morphology of lipid domains in an environment similar to that found in cells.

MATERIALS AND METHODS

Materials

Laurdan and *N*-Rh-DPPE were from Molecular Probes (Eugene, OR). 1-Palmitoyl, 2-oleoyl-*sn*-glycero-3-phosphocholine (POPC), DLPC, DMPC, DPPC, DSPC, and 1,2-diarachidoyl-*sn*-glycero-3-phosphocholine (DAPC) were from Avanti Polar Lipids (Alabaster, AL) and were used without further purification.

Methods

Vesicle preparation

Stock solutions of phospholipids were made in chloroform. The concentration of the lipid stock solutions was 0.2 mg/ml. For GUV preparation we followed the electroformation method developed by Angelova and Dimitrov (Angelova and Dimitrov, 1986; Dimitrov and Angelova, 1987; Angelova et al., 1992). To prepare the GUVs, a special temperature-controlled chamber, which was previously described (Bagatolli and Gratton, 1999, 2000), was used. The following steps were used: 1) ~3 μl of the lipid stocks solution were spread on each Pt wire under a stream of N_2. To remove the residues of organic solvent, the samples were lyophilized for ~2 h; 2) To add the aqueous solvent inside the chamber (Millipore water 17.5 MΩ/cm), the bottom part of the chamber was sealed with a coverslip. The water was previously heated to temperatures corresponding to the fluid phase (above the lipid mixture phase transitions), and then sufficient water was added to cover the Pt wires (~5 ml). Just after this step the Pt wires were connected to a function generator (Hewlett-Packard, Santa Clara, CA), and a low-frequency AC field (sinusoidal wave function with a frequency of 10 Hz and an amplitude of 2 V) was applied for 90 min. After the vesicle formation, the AC field was turned off and the temperature scan (from high to low temperatures) was initiated. The experiments were carried out in the same chamber after the vesicle formation, using an inverted microscope (Axiovert 35; Zeiss, Thornwood, NY). Specifically, the images of the GUVs were obtained in the chamber, using the Pt wires as a "holder," as previously reported (Bagatolli and Gratton, 1999, 2000). The vesicles are attached to the Pt wires, which are covered by a lipid film. This fact allows us to make temperature scans of targeted single GUVs without vesicle drifting. A CCD color video camera (CCD-Iris; Sony) in the microscope was used to follow vesicle formation and to select the target vesicle. The temperatures we used for GUVs formation were 70°C for the DLPC/DAPC (1:1 mol/mol) mixture, 60°C for DMPC/DSPC and DLPC/DSPC (1:1 mol/mol) mixtures, 55°C for DMPE/DMPC (7:3 mol/mol), and 50°C for the DLPC/DPPC (1:1 mol/mol) mixture. The temperature was measured inside the sample chamber, using a digital thermocouple (model 400B; Omega, Stamford, CT) with a precision of 0.1°C. The Laurdan labeling procedure was done in one of two ways. Either the fluorescent probe was premixed with the lipids in chloroform or a small amount (less than 1 μl) of Laurdan in dimethyl sulfoxide was added after the vesicle formation (final Laurdan/lipid ratio, 1:500 mol/mol in both cases). The sample behavior during the temperature scan was independent of the labeling procedure. In the case of *N*-Rh-DPPE the lipid was premixed with the fluorescent phospholipid in chloroform. The percentage of *N*-Rh-DPPE in the sample was less than 0.5 mol%. We note that the presence of *N*-Rh-DPPE dimers, i.e., nonfluorescent rhodamine complexes, is unlikely at the low probe concentration utilized in the experiments. The GUV yield was ~95%, and the mean diameter of the GUVs was ~30 μm. To check the lamellarity of the giant vesicles we imaged several vesicles (up to 20 vesicles in different regions of the Pt wires) labeled with Laurdan or *N*-Rh-DPPE, using the two-photon excitation microscope. We found that the intensities measured in the border of different vesicles in the liquid crystalline phase were very similar. Because the existence of multilamellar vesicles would give rise to different intensity images due to the presence of different numbers of Laurdan-labeled lipid bilayers, we concluded that the vesicles were unilamellar, in agreement with previous observations of GUVs made by the electroformation method (Mathivet et al., 1996; Bagatolli and Gratton, 1999, 2000; Bagatolli et al., 2000).

Two-photon fluorescent measurements

Experimental apparatus for two-photon excitation microscopy measurements. Two-photon excitation is a nonlinear process in which a fluorophore absorbs two photons simultaneously. Each photon provides half the energy required for excitation. The high photon densities required for two-photon absorption are achieved by focusing a high peak power laser light source on a diffraction-limited spot through a high numerical aperture objective. Therefore, in the areas above and below the focal plane, two-photon absorption does not occur, because of insufficient photon flux. This phenomenon allows for a sectioning effect without the use of emission pinholes as in confocal microscopy. Another advantage of two-photon excitation is the low extent of photobleaching and photodamage above and below the focal plane. For our experiments we used a scanning two-photon fluorescence microscope developed in our laboratory (So et al., 1995, 1996). We used an LD-Achroplan 20× long working distance air objective (Zeiss, Holmdale, NJ) with a NA of 0.4. A titanium-sapphire laser (Mira 900; Coherent, Palo Alto, CA) pumped by a frequency-doubled Nd:vanadate laser (Verdi; Coherent) was used as the excitation light source. The excitation wavelength was set to 780 nm. The laser was guided by a galvanometer-driven *x*-*y* scanner (Cambridge Technology, Watertown, MA) to achieve beam scanning in both the *x* and *y* directions. The scanning rate was controlled by the input signal from a frequency synthesizer (Hewlett-Packard, Santa Clara, CA), and a frame rate of 25 s was used to acquire the images (256 × 256 pixels). The laser power was attenuated to 50 mW before the light entered the microscope. The samples received ~1/10 of the incident power. To change the polarization of the laser light from linear to circular, a quarter-wave plate (CVI Laser Corporation, Albuquerque, NM) was placed before the light entered the microscope. The fluorescence emission was observed through a broad band-pass filter from 350 nm to 600 nm (BG39 filter; Chroma Technology, Brattleboro, VT). A miniature photomultiplier (R5600-P; Hamamatsu, Bridgewater, NJ) was used for light detection in the photon counting mode. A home-built card in a personal computer acquired the counts. The diameters of the vesicles were measured by using size-calibrated fluorescent spheres (latex FluoSpheres, polystyrene, blue fluorescent 360/415, diameter 15.5 μm; Molecular Probes). We determined that the pixel size in our experiments corresponds to 0.52 μm.

GP function. Laurdan's emission spectrum is blue in the lipid gel phase, while in the liquid crystalline phase it moves during the excited-state lifetime from blue to green (Parasassi et al., 1990, 1991). To quantify the

emission spectral changes, the excitation GP function was defined analogously to the fluorescence polarization function as

$$GP = \frac{I_B - I_R}{I_B + I_R}$$

where I_B and I_R correspond to the intensities at the blue and red edges of the emission spectrum (respectively), using a given excitation wavelength (Parasassi et al., 1990, 1991). This well-characterized function is sensitive to the phase state of lipid aggregates (for reviews see Parasassi and Gratton, 1995; Parasassi et al., 1998). For the Laurdan GP measurements we used a procedure similar to that previously described (Yu et al., 1996; Parasassi et al., 1997; Bagatolli and Gratton, 1999, 2000). The Laurdan GP function on the GUVs images was computed using two Laurdan fluorescence images, one obtained in the blue (I_B) and other obtained in the green (I_R) regions of the Laurdan emission spectrum. To obtain these Laurdan fluorescence images for GP calculation, two optical bandpass filters, in addition to the BG39, centered at (446 ± 23) nm (I_B) and at (499 ± 23) nm (I_R) (Ealing Electro-optics, New Englander Industrial Park, Holliston, MA), were used on the microscope.

Laurdan: photoselection effect and lipid phase-dependent spectral shift. In a previous study, Parasassi et al. showed that polarized light excitation of Laurdan-labeled multilamellar vesicles caused a photoselection effect in the fluorescence emission image (Parasassi et al., 1997). This effect was recently confirmed in GUVs composed of pure phospholipid and phospholipid binary mixtures (Bagatolli and Gratton, 1999, 2000). The electronic transition dipole of Laurdan in lipid vesicles is aligned parallel to the hydrophobic lipid chains (Parasassi and Gratton, 1995; Parasassi et al., 1998; Bagatolli and Gratton, 1999, 2000). Consider a circular polarization confined to the *x-y* plane. By exploring different regions of a spherical vesicle (at a given vertical section) we can observe that the strong excitation occurs in the regions where Laurdan's dipole is aligned parallel to the polarization plane of the excitation light. Observing the top or bottom regions of a spherical lipid vesicle, we will find lower excitation compared with that obtained at the center region of the vesicle (see Fig. 1). This last observation is explained by the fact that Laurdan's dipoles in the top or the bottom regions of the vesicles are located mainly perpendicular to the plane of the polarization of the excitation light (Fig. 1). In addition, the photoselection effect depends on the phase state of the phospholipids. In the fluid phase we always expect to have a component of Laurdan's transition dipole parallel to the excitation polarization because of the relatively low lipid order. As a consequence of the reduced order, there is less difference in the emission intensity between the parallel and perpendicular orientations of Laurdan's electronic transition dipole compared with that obtained in the gel phase (Fig. 1) (Parasassi et al., 1997; Bagatolli and Gratton, 1999). In the gel phase the packing of the lipid molecules is very tight, increasing the photoselection effect (see Fig. 1) (Parasassi et al., 1997; Bagatolli and Gratton, 1999, 2000). As a consequence, the images taken at the top or bottom regions of the vesicle will show no intensity (Fig. 1). On the other hand, we want to remark again that Laurdan's emission is blue (the emission maximum will be located at ~ 440 nm) in the gel phase and green (the emission maximum will be located at ~ 490 nm) in the fluid phase.

The above findings provide important tools for discriminating between fluid and solid domains at the phase coexistence temperature when the intensity images are taken at top (or bottom) and center regions of the Laurdan-labeled GUVs. We want to point out that Laurdan is homogeneously distributed between the solid and fluid lipid phases (Parasassi et al., 1991; Bagatolli and Gratton, 2000). Therefore, when the lipid domains are larger than the image pixel size and circular polarization in the excitation light is used, 1) we can differentiate solid and fluid lipid domains in the top of the vesicle because the solid domains are nonfluorescent and the fluid domains are fluorescent (photoselection effect); 2) in the equatorial region of the vesicle we can differentiate between the solid and fluid domains because the emission spectra of Laurdan are different (blue and green light, respectively; see Fig. 1). In this last case we compute the differences between the fluid and solid lipid domains, using the GP function. When the sizes of the lipid domains are equal to or smaller than the image pixel size, the linear polarization in the excitation light is more effective in ascertaining domain coexistence (Parasassi et al., 1997; Bagatolli and Gratton, 1999, 2000). The linear polarization in the excitation light, which photoselects well-oriented Laurdan molecules, also selects Laurdan molecules associated with a high GP value (Parasassi et al., 1997; Bagatolli and Gratton, 1999). In linear polarized excitation light, if the image contains separate domains (pixels) of different GP values, the higher

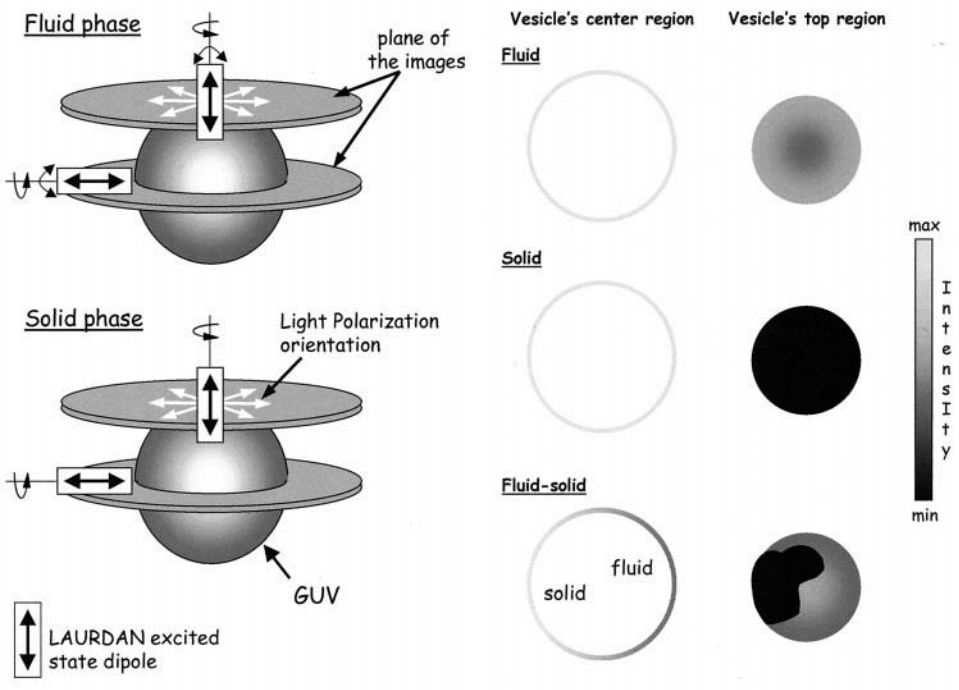

FIGURE 1 Schematic representation of the photoselection effect, using circular polarized excitation light on the Laurdan-labeled GUV fluorescence intensity images. The small double-headed curved arrows associated with the Laurdan excited state dipoles in the fluid phase (*upper left*) denote probe mobility (wobbling), which dramatically decreases in the solid phase.

GP value domains appear parallel to the direction of the polarization of the excitation light (Parasassi et al., 1997; Bagatolli and Gratton, 1999, 2000).

N-Rh-DPPE probe: photoselection effect and differential probe partition. A different situation was found using *N*-Rh-DPPE. The excited-state dipole of this probe is aligned perpendicular to the surface of the GUVs (Bagatolli and Gratton, 2000). In addition, using linear polarized excitation light, we observed that this probe does not show intensity dependence with the lipid packing (not shown), as demonstrated previously for Laurdan (Bagatolli and Gratton, 1999). Specifically, the difference in the emission intensity between the parallel and perpendicular orientations of the *N*-Rh-DPPE excited-state dipole, with respect to the orientation of the linear polarized light, is independent of the lipid phase state. Using circular polarized light, and as a consequence of the location of the *N*-Rh-DPPE excited-state dipole in the membrane, the fluorescence intensity in the top or center region of a single-component GUV is not affected by the lipid phase state, as we reported for Laurdan (compare Figs. 1 and 2). However, for phospholipid binary mixtures we reported that the coefficient for the partition of *N*-Rh-DPPE to the different lipid phases depends on the lipid binary mixture characteristics (Bagatolli and Gratton, 2000). For example, at the phase coexistence temperature regime we found that *N*-Rh-DPPE is completely segregated from the DPPE gel domains in DPPE/DPPC mixtures (Fig. 2). In contrast to the last observation and at the phase coexistence temperature regime *N*-Rh-DPPE showed high affinity for the more ordered lipid domains in DPPC/DLPC mixtures (Fig. 2; Bagatolli and Gratton, 2000).

To summarize, we are able to discriminate between fluid and solid domains at the phase coexistence temperature regime by using *N*-Rh-DPPE because the concentration of the probe is different between the solid and fluid phases. We want to remark that the last phenomenon is different from that found for Laurdan, in which the probe partition is independent of the lipid phase state (Bagatolli and Gratton, 2000).

RESULTS

DLPC-containing GUVs

Images of *N*-Rh-DPPE-labeled GUVs composed of DLPC/DPPC, DLPC/DSPC, and DLPC/DAPC (1:1 mol/mol in all cases) at temperatures corresponding to the fluid phase and fluid-solid phase coexistence are shown in Fig. 3. These images were taken at the vesicle's top or bottom regions. At temperatures corresponding to the fluid phase we observed a homogeneous distribution of the fluorescent molecules (Fig. 3, *A–C*). In all cases, as the temperature was decreased we detected a particular temperature for each lipid mixture at which distinct areas become visible on the vesicle surface showing lipid domain coexistence. The temperatures for the fluid→fluid-solid phase transition determined from the images were 36°C for DLPC/DPPC, 48°C for DLPC/DSPC, and 63°C for DLPC/DAPC. The transition temperatures of the high melting component for DLPC/DSPC and DLPC/DPPC (1:1 mol/mol) are in agreement with that previously reported (Mabrey and Sturtevant, 1976; Bagatolli and Gratton, 2000). To our knowledge there is no phase diagram reported in the literature for the DLPC/DAPC mixture to compare with our data. All of these samples display concurrent fluid and solid domains over the temperature range tested (lower temperature: 10°C). Fig. 3, *D–F*, shows different solid domain shapes, depending on the binary mixture composition. DLPC/DPPC shows line shapes in agreement with previous data (Fig. 3 *D*) (Bagatolli and Gratton, 2000). The domains found in DLPC/DSPC have a quasicircular shape (Fig. 3 *E*). There is a high occurrence rate of these quasicircular shape domains (~95% of the overall lipid sample) with low percentages of line shape domains. In the case of DLPC/DAPC the solid domains showed a dendritic shape (Fig. 3 *F*). In all cases after the transition of the high melting lipid component, the lipid solid domains expanded and migrated around the vesicle surface as we decreased the temperature. However, the mobility of the lipid domains is grad-

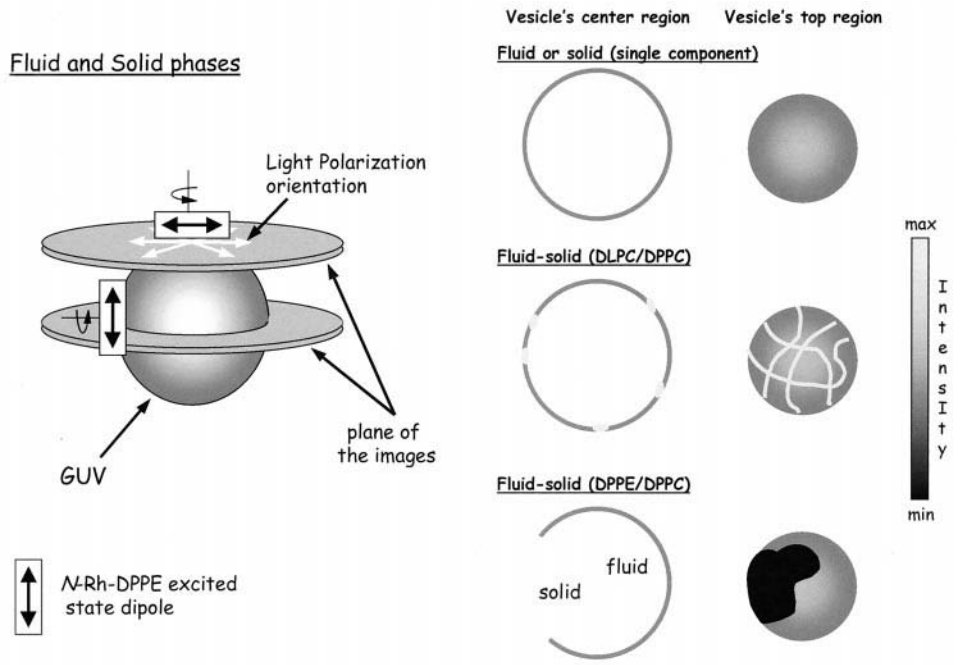

FIGURE 2 Schematic representation of the photoselection effect, using circular polarized excitation light and the probe partition on *N*-Rh-DPPE-labeled GUV fluorescence intensity images. The small curved arrows associated with the *N*-Rh-DPPE excited-state dipoles in the fluid phase (*upper left*) denote probe mobility (rotation), which decreases in the solid phase. The wobbling movement of the probe is not indicated in the figure.

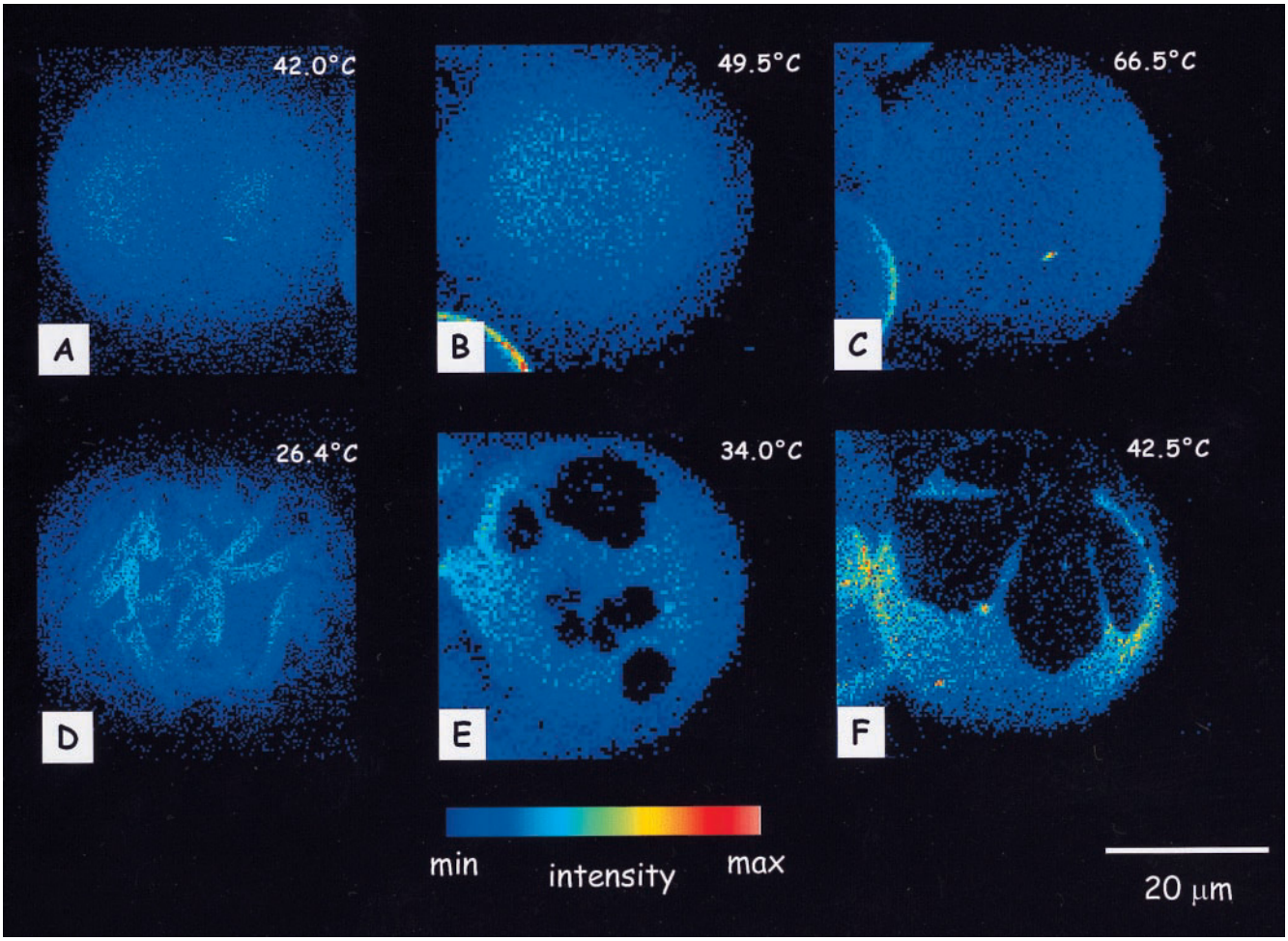

FIGURE 3 Two-photon excitation fluorescence intensity images (false color representation) of GUVs formed of DLPC/DPPC (*A* and *D*), DLPC/DSPC (*B* and *E*), and DLPC/DAPC (*C* and *F*) (1:1 mol/mol), labeled with *N*-Rh-DPPE. The images have been taken at the top part of the GUV at temperatures corresponding to the fluid phase (*A–C*) and the fluid-solid phase coexistence (*D–F*).

ually reduced as the temperature decreases. The sizes of the domains were on the order of several microns (up to ~30 μm). An interesting feature connected to the lipid domain characteristic was observed: at temperatures corresponding to phase coexistence, the nonfluorescent areas in the GUV span the lipid membrane (Fig. 3).

Using Laurdan, we observed similar domain shapes in the top region of the different DLPC-containing GUVs (not shown) compared with those obtained with *N*-Rh-DPPE. This last result is in agreement with the observation from our previous work, in which the shape of the solid lipid domain is independent of the fluorescent molecule used in the experiments (Bagatolli and Gratton, 2000). The phase state of the lipid domains in the different mixtures was determined using the GP function. For all mixtures, the GP histograms were fit with a Gaussian function, showing a single broad component at temperatures corresponding to the fluid phase (~ −0.2, not shown) and a bimodal histogram at temperatures corresponding to the phase coexistence region (high and low GP). Fig. 4 shows Laurdan's GP images at the center cross section of the different DLPC-containing GUVs at the phase coexistence temperature regime and the corresponding fitted GP histograms. In this temperature regime, the difference between the centers of the Laurdan GP histogram (for the low and high GP components) among the different binary mixtures increases in the following order: DLPC/DPPC < DLPC/DSPC < DLPC/DAPC (Fig. 4 and Table 1). We found that the center values of the GP histograms and the difference between the hydrophobic chain lengths of the components of the phospholipid mixture exhibit a linear relationship (Fig. 5). We want to remark that the center values of the Laurdan GP histograms for the solid and fluid components for the DLPC/DAPC mixture resemble those obtained in the fluid and gel phases in GUVs composed of a pure phospholipid (Bagatolli and Gratton, 1999). This finding shows that the

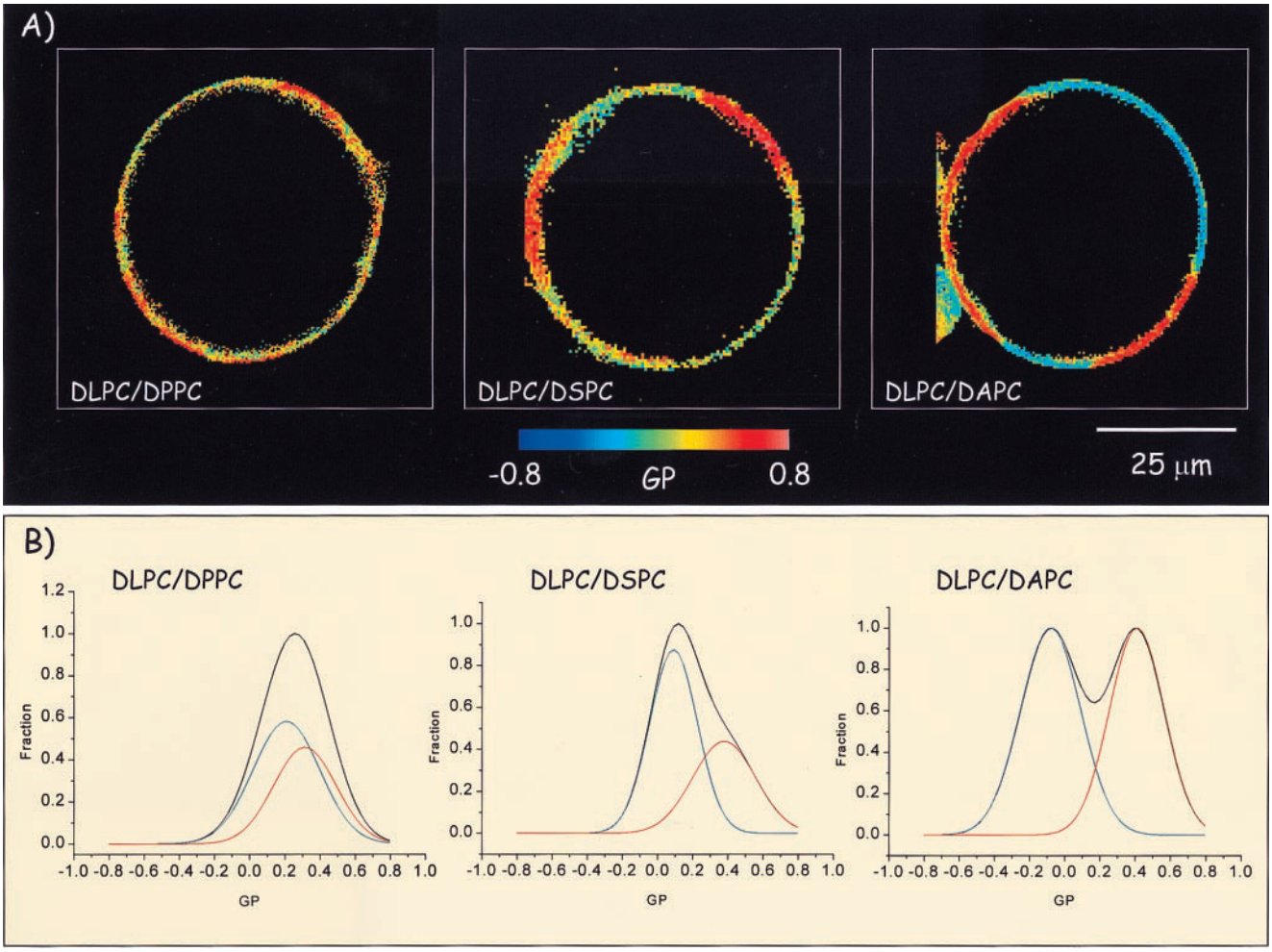

FIGURE 4 (*A*) Two-photon excitation Laurdan GP images of a single GUV composed of DLPC/DPPC, DLPC/DSPC, and DLPC/DAPC (1:1 mol/mol in all cases) obtained with circular polarization light. (*B*) Fitted GP histograms corresponding to the three images presented in *A*. For the fitting procedure we used Gaussian functions. For comparison, the Laurdan GP images were taken at temperatures 8°C below the fluid→fluid-solid phase transition (28°C for DLPC/DPPC, 40°C for DLPC/DSPC, and 55°C for DLPC/DAPC).

domain coexistence in DLPC/DAPC is between pure fluid and pure gel lipid domains, as we found in the DPPE/DPPC (7:3 mol/mol) mixture (Bagatolli and Gratton, 2000).

DMPC/DSPC and DMPE/DMPC mixtures

In the fluid phase the images obtained with *N*-Rh-DPPE or Laurdan for both mixtures (DMPC/DSPC 1:1 mol/mol and DMPE/DMPC 7:3 mol/mol) show that the fluorescent molecules are distributed homogeneously on the vesicle surface (Fig. 6). As the temperature was decreased, at 48.2°C for the DMPC/DSPC mixture and 49.0°C for the DMPE/DMPC mixture, nonfluorescent areas become visible on the vesicle surface showing lipid domain coexistence (Fig. 6). The temperature for the fluid→fluid-solid phase transition determined from the images for the DMPC/DSPC mixture is in agreement with the phase diagram of the mixture (Mabrey and Sturtevant, 1976). The concurrent fluid and solid domains in the DMPC/DSPC mixture are present on the vesicle surface from 48.2 to 28.0°C. The solid domains in the DMPC/DSPC mixture have a particular aspect, i.e., a combination of an amorphous nonfluorescent central region with nonfluorescent extensions (Fig. 6 *A*). In this case we also observed the nonfluorescent regions spanning the lipid membrane (Fig. 6 *a*). From 48.2 to 28.8°C the nonfluorescent regions expanded and migrated around the vesicle surface as

TABLE 1 Centers of the Laurdan histogram

Lipid mixture (1:1 mol/mol)	ΔCH_2	GP histogram center (fluid-solid phase coexistence)	
DMPC/DSPC	4	0.20	0.33
DLPC/DPPC	4	0.18	0.31
DLPC/DSPC	6	0.05	0.38
DLPC/DAPC	8	−0.08	0.49

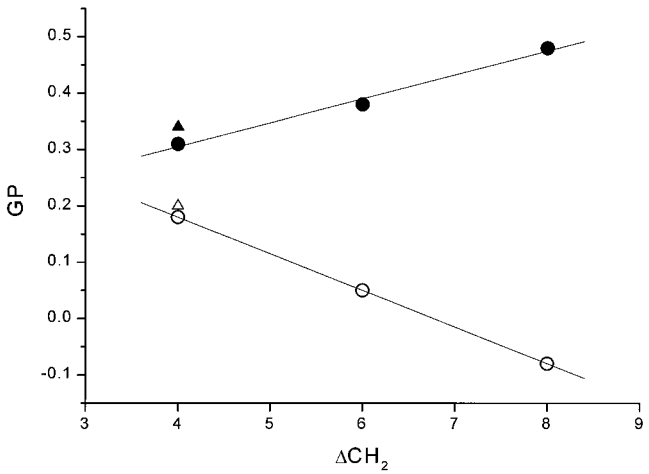

FIGURE 5 Laurdan GP versus the CH_2 difference between the hydrophobic chain lengths of the different PC binary mixtures. The open and solid symbols denote fluid and solid domains, respectively. ○, ●, DLPC-containing GUVs; ▲, △, DMPC/DSPC mixture.

the temperature was decreased. However, the mobility of the lipid domains is gradually reduced as the temperature decreases. The size of the nonfluorescent domains was on the order of several microns. Below 28.8°C, the nonfluorescent regions gradually disappear, showing, at 26.0°C, an almost homogeneous fluorescence distribution on the vesicle surface (Fig. 6 *A*). This finding suggests lipid miscibility at the solid-solid temperature regime. However, some small nonfluorescent domains remain on the vesicle surface.

In the case of the DMPE/DMPC (7:3 mol/mol) mixture at the phase coexistence temperature regime, the solid domains are nonfluorescent and present a dendritic shape (Fig. 6 *B*). The solid domains expanded and migrated around the vesicle surface as the temperature was decreased. Below 26.5°C the mobility of the nonfluorescent domains decreases dramatically. Large size nonfluorescent domains remain on the GUV surface at low temperatures (we examined them up to 15°C; Fig. 6 *B*), in contrast to that observed for DMPC/DSPC mixture. In either the solid-fluid or solid temperature regime the lipid domains span the lipid bilayer. The general behavior of GUVs composed of DMPE/DMPC mixture is in keeping with that obtained for the DPPE/DPPC (7:3 mol/mol) mixture (Bagatolli and Gratton, 2000).

The GP histogram in the three different temperature regimes, together with the GP images at the phase coexistence temperature regime for both DMPC/DSPC and DMPE/DMPC mixtures, is shown in Fig. 7. In GUVs composed of the DMPC/DSPC (1:1 mol/mol) mixture in the fluid phase (60.2°C) a broad GP histogram center at −0.18 was obtained (Fig. 7 *A*). At the phase coexistence temperature regime DMPC/DSPC shows a bimodal distribution presenting a small separation between the GP values of the solid and fluid domains (Table 1 and Fig. 7 *A*). Below 28.8°C, which corresponds to the solid-fluid→solid phase transition determined from the GP experiments, the GP histogram is narrow and is centered at 0.53 (Fig. 7 *A*). For DMPE/DMPC at temperatures corresponding to the fluid phase (60.0°C) the histogram is broad and is centered at −0.02 (Fig. 7 *B*). When this sample presents a solid-fluid domain coexistence the GP histogram is bimodal, showing a large separation between the GP centers of the fluid and solid components (0.15 and 0.5, respectively). Below 26.5°C, which corresponds to the solid-fluid→solid phase transition determined form the GP experiments, the GP histogram is narrow and is centered at 0.54.

DISCUSSION

Fluid-phase temperature regime

Although we observed a homogeneous fluorescence distribution on the GUV surface, using either Laurdan or *N*-Rh-DPPE, we found that the Laurdan GP histogram in the fluid phase is particularly broad (compared with that obtained in the solid phase; see, for example, Fig. 7 *B*). This extensive GP heterogeneity found in the fluid phase of the binary mixtures does not correlate with images presenting large domains (micron-size domains), as we observe in the fluid-solid temperature regime, using the two-photon excitation fluorescence images. This heterogeneity of the GP histograms was previously observed at the fluid phase temperature regime in GUVs composed of single components and binary mixtures (Bagatolli and Gratton, 1999, 2000) and in multilamellar vesicles composed of DOPC or DLPC (Parasassi et al., 1997). Using linear polarized light as an excitation source, previous studies have reported a separation of low and high GP regions in the fluorescence images (Parasassi et al., 1997; Bagatolli and Gratton, 1999, 2000). In all of these cases, the different GP domains in the fluid phase were smaller than the microscope resolution (Parasassi et al., 1997; Bagatolli and Gratton, 1999, 2000), in keeping with our results. To understand these observations, it is important to recall that Laurdan is sensitive to the water content in phospholipid interfaces (Parasassi and Gratton, 1995; Parasassi et al., 1998). To explain the observed heterogeneity in the GP histogram, Parasassi et al. proposed the following model. In the fluid phase there is a distribution of sites with different sizes in which the Laurdan molecule can reside (Parasassi et al., 1997). The more water molecules in the site the lower the GP value and the larger the cavity around the Laurdan molecule (Parasassi et al., 1997). From the model and the GP histograms it is clear that the fluid phase presents a nonrandom organization in agreement with previous observations (Jørgensen et al., 1993; Mouritsen, 1998).

Using computer simulation, Jørgensen et al. compared the lipid organization of different nonideal phosphatidylcholine binary mixtures in the fluid phase (Jørgensen et al., 1993). When the hydrophobic mismatch is eight carbons (DLPC/DAPC), these authors find that the fluid phase

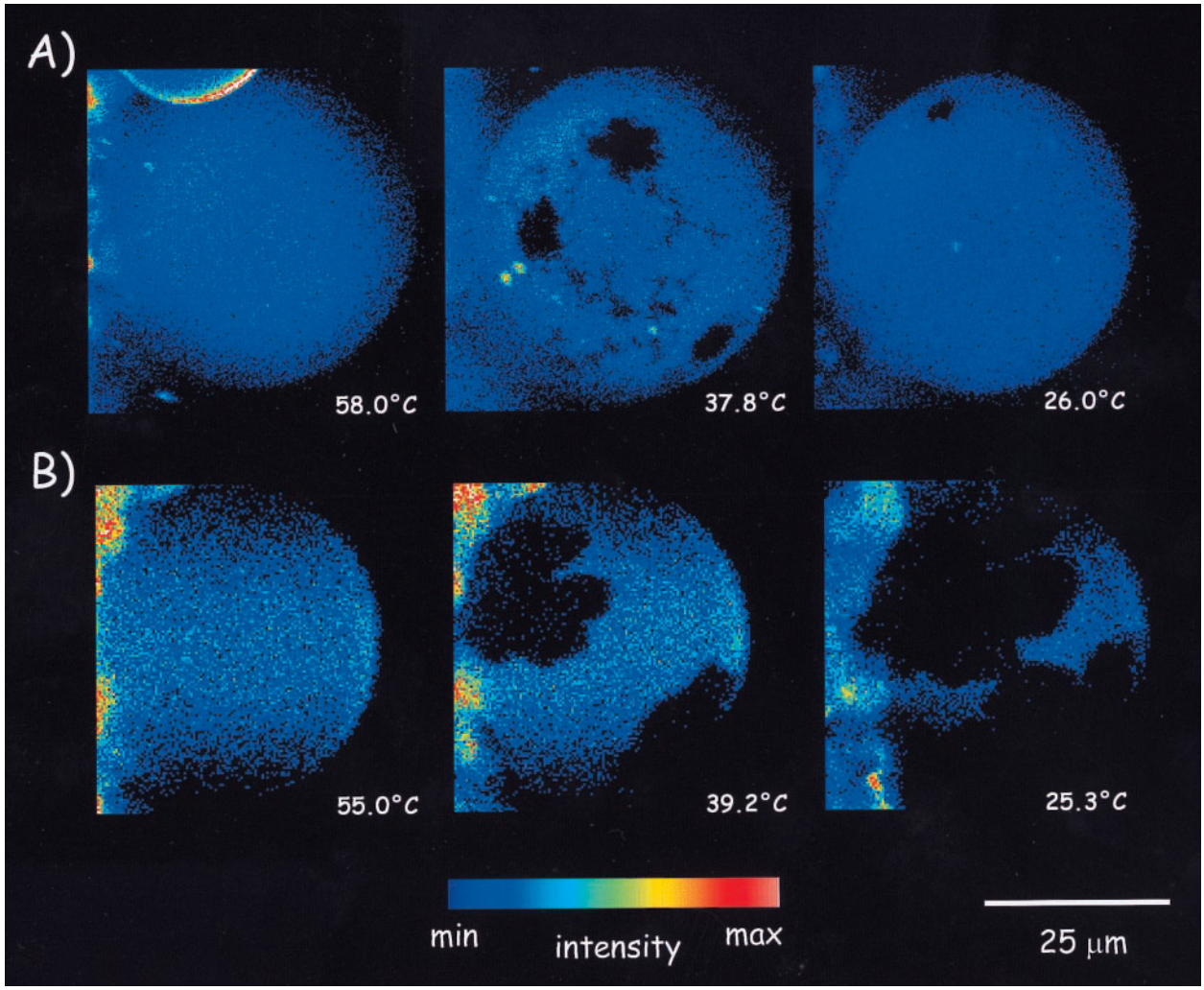

FIGURE 6 Two-photon excitation fluorescence intensity images (false color representation) of GUVs formed of DMPC/DSPC (*A*) and DMPE/DMPC (*B*) (1:1 and 7:3 mol/mol, respectively), labeled with *N*-Rh-DPPE. The images have been taken at the top part of the GUV at the fluid, fluid-solid, and solid-solid temperature regimes. In the case of DMPC/DSPC the solid domains gradually disappear below 28.8°C.

shows a strong tendency for clustering of like lipids in a way that resembles microphase separation (Jørgensen et al., 1993). These authors also found that this last effect is less pronounced in DLCP/DSPC mixtures and even less so in DMPC/DSPC mixtures (Jørgensen et al., 1993). On the other hand, Gliss et al. found no presence of domains in the fluid phase of DMPC/DSPC (1:1 mol/mol), using grazing incidence neutron diffraction and atomic force microscopy (Gliss et al., 1998). Even though we found microheterogeneity in the fluid phase for DLPC/DPPC, DLPC/DSPC, DLPC/DAPC, and DMPC/DSPC (1:1 mol/mol) mixtures, we did not observe differences among the GP histograms of these mixtures in the fluid phase. However, we found that the GP center value for DMPE/DMPC (7:3 mol/mol) in the fluid phase is higher than that found for the GUVs composed of PC-containing binary mixtures (see, for example, Fig. 7 *B*). This difference was also observed between DPPE/DPPC (7:3 mol/mol) and DLPC/DPPC (1:1 mol/mol) mixtures (Bagatolli and Gratton, 2000). The observed differences between the PC- and PE/PC-containing binary mixtures in the fluid phase can be explained by taking into account the effect caused by the low hydration of the PE polar headgroup compared with PC (Boggs, 1987), or there may be some differences in the microphase separation between these mixtures in the fluid phase.

Solid-fluid phase coexistence temperature regime

A common feature on the two-photon excitation fluorescence images concerns the symmetry of the solid domains along the normal to the bilayer surface. Independent of the lipid sample and the fluorescent probe, our images show a

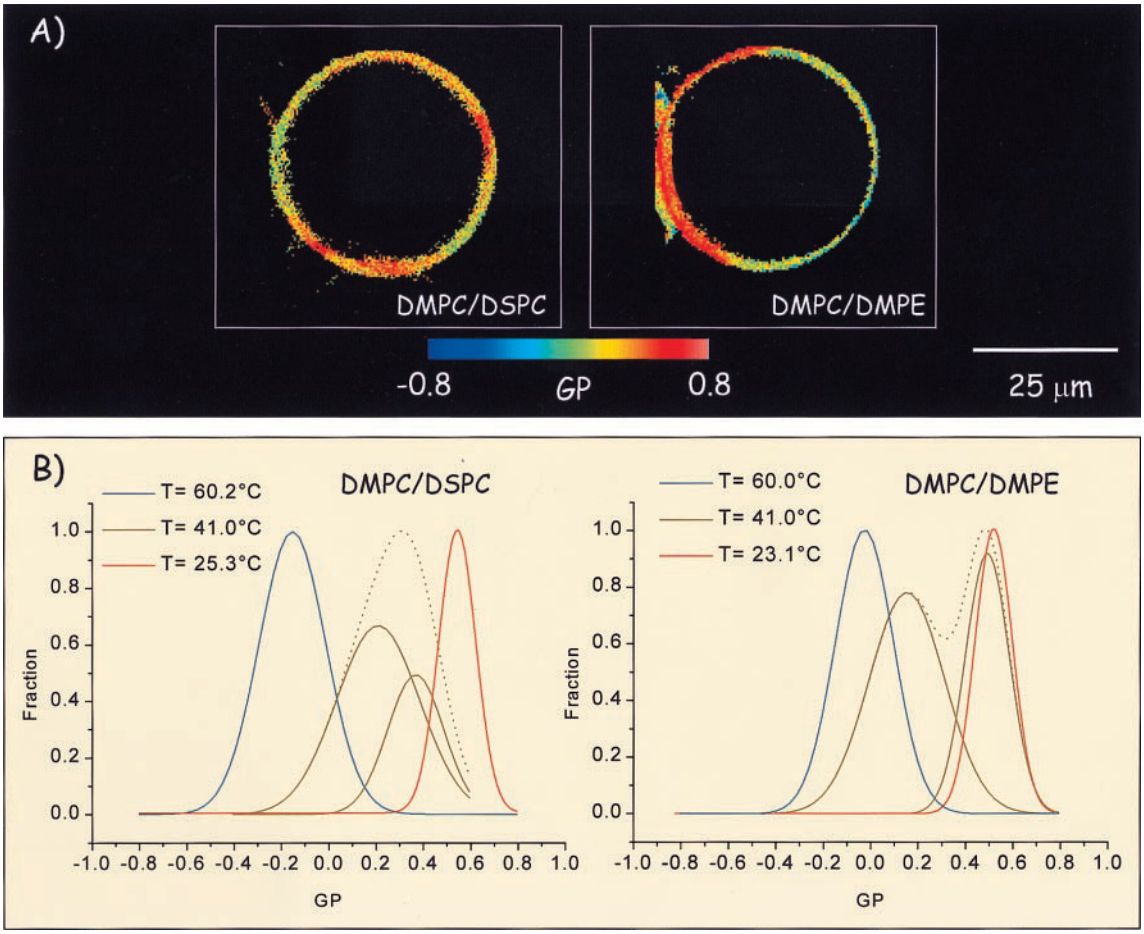

FIGURE 7 (*A*) Two-photon excitation Laurdan GP images of a single GUV composed of DMPE/DMPC (7:3 mol/mol) and DMPC/DSPC (1:1 mol/mol) obtained with circular polarization light at 41°C. (*B*) Fitted GP histograms corresponding to the three different temperature regimes (fluid, fluid-solid, and solid-solid) for DMPE/DMPC (7:3 mol/mol) and DMPC/DSPC (1:1 mol/mol). For the fitting procedure we used Gaussian functions.

coupling between the inner and outer leaflets of the bilayer. This last finding extends previous observations made in work on GUVs composed of binary mixtures (DPPE/DPPC and DLPC/DPPC) (Bagatolli et al., 1999; Bagatolli and Gratton, 2000) and in mixtures of DLPC/DPPC/POPS and DLPC/DPPC/POPS/cholesterol, using confocal microscopy (Korlach et al., 1999). Because these observations were made in different lipid mixtures we conclude that the coupling between the inner and outer leaflets of the bilayer at the phase coexistence temperature regime is a general phenomenon in samples that display solid-fluid phase coexistence. This phenomenon should be taken into account in theoretical models and computer simulations. As we pointed out in our previous work, it could be possible that the molecular arrangement of the lipid molecules in the gel phase enhances the phospholipid tail-tail interaction (Bagatolli and Gratton, 2000). These tail-tail interactions could drive the formation of lipid cluster from one side of the bilayer plane to the other. This important observation, i.e., the fact that the solid domains span the lipid bilayer, confirms the existence of epitactic coupling in free-standing bilayers. Direct epitactic coupling has also been demonstrated in studies of supported membranes by Merkel et al. (1989), where it was shown that solid domains in one monolayer induce the solidification of domains of identical topology in juxtaposed monolayers transferred from the fluid state.

Correlation between solid domain geometry and binary mixture composition.

To investigate the relationship between the geometry of the solid domains and the chemical nature of the binary mixture components, we investigated different mixtures containing DLPC at the phase coexistence temperature regime. Considering this saturated binary mixture series, we showed that the geometry of the solid domains changes from a line shape to a quasicircular shape to finally adopt a dendritic shape, as the hydrophobic mismatch in the binary mixture increases.

What process causes the change in the geometry of the lipid domain in the series of DLPC-containing mixtures? A computer simulation analysis comparing nonideal PC binary mixtures at the phase coexistence region was reported in the literature (Jørgensen et al., 1993). These authors found an interesting phenomenon of local interfacial ordering called interfacial wetting. In DLPC/DSPC (1:1 mol/mol) mixtures they found that in the phase coexistence region a layer of gel-type acyl chain configurations of the low melting component (DLPC) wetted the gel phase mainly formed by DSPC. This layer, which extends over several acyl chain diameters for the DLPC/DSPC mixture, is not a static entity but is dynamically maintained. These authors also found that the wetting effect is less pronounced in DMPC/DSPC compared with DLPC/DSPC, i.e., it is dependent on the degree of nonideality of the mixture (Jørgensen et al., 1993). A consequence of the wetting effect is the lowering of the interfacial tension in the solid domain borders, which implies a slowing down of the interfacial dynamics and an increase in the lifetime of the local structure (Jørgensen et al., 1993). We believe that this phenomenon can be important in explaining the changes in the domain geometry with an increase in the mixture nonideality. We believe that the lipid composition on the domain boundary regions may affect the lipid long-range interactions influencing a particular solid domain shape. A very peculiar case is the difference in the solid domain geometry at the phase coexistence temperature regime observed between the DMPC/DSPC and DLPC/DPP (1:1 mol/mol) mixtures (compare Figs. 3 and 6). For these two mixtures we found comparable Laurdan GP histograms at the phase coexistence temperature regime, suggesting similar pictures of the fluid-solid domain coexistence. These two binary mixtures present the same hydrophobic mismatch, but their extents of nonideality are different, as judged from the phase diagrams (Van Dijck et al., 1977; Mabrey and Sturtevant, 1976). Further experiments are needed to clarify this difference. For the moment we believe that the lipid compositions at the domain borders for these two samples should be different, influencing the domain geometry.

The same dendritic shape of the solid domains obtained in GUVs composed of DPPE/DPPC (7:3 mol/mol) was observed in the DMPE/DMPC (7:3 mol/mol) mixture and the DLPC/DAPC (1:1 mol/mol) mixture. In addition to the similarity of the solid domain geometry among these three different mixtures, the Laurdan GP measured in the fluid and solid domains resembles those of the pure fluid and pure gel of single-component phospholipid GUVs (Bagatolli and Gratton, 1999). Therefore, the geometry and phase state of the solid domains are the same, independently of the characteristics of the phospholipid components among these mixtures. An important point here is that either the difference between the polar headgroups or that between the hydrophobic chain lengths for the binary mixture components can independently cause the fluid-solid domain coexistence with very similar topological features.

The link between the shape and size of the liquid condensed domains in monolayers and the domains found in the binary mixtures provides an important point of comparison between these two systems. An important point is that the curvature radius of the GUVs is very low compared with those found in small or large unilamellar vesicles and closer to that of lipid monolayers. This similarity can be important in explaining the matching size and shape among lipid domains found in GUVs and monolayers. As an example, the size and shape of the solid domains found at the phase coexistence temperature regime in GUVs composed of DLPC/DAPC, DMPE/DMPC, and DPPE/DPPC (Bagatolli and Gratton 2000) are similar to those found in monolayers of DPPE at the liquid expanded/liquid condensed phase coexistence region (Grainger et al., 1990). In recent years a great variety of domain shapes in monolayer systems has been described in the literature (Weis and McConnell, 1985; Grainger et al., 1990; Möhwald et al., 1995, and references therein). Theoretical models that consider the effect of long-range electrostatic interactions and line tension at the boundary of lipid domains on the shape of large (i.e., micron size) lipid domains have been reported for lipid monolayers (Möhwald et al., 1995; for a review see Raudino, 1995). For lipid bilayers displaying lipid phase separation Sackmann and Feder introduced a model that combines the theory of spinoidal decomposition and the membrane bending energy concept (Sackmann and Feder, 1995). These authors show different domain shapes obtained by electron microscopy as stripelike arrangements of two-dimensional precipitates and hexagonal arrangements of circular domains, both predicted by the theory. They also mention that plane-wave domains have been obtained in membranes exhibiting gel-fluid coexistence, whereas circular domains are commonly observed in cases of fluid-fluid demixing (Sackmann and Feder, 1995). We observed a great variety of large domain shapes in free bilayers composed of binary mixtures (several orders of magnitude larger than that reported from electron microscopy studies or from computer simulations). We believe that our experimental information will be useful for future theoretical models.

Phase state of lipid domain measured by the Laurdan GP function

For DLPC-containing GUVs at the phase coexistence temperature regime, the differences between the high and low GP center values for each binary mixture increase as the difference in the number of methylenes between the hydrophobic chains of DLPC and the second phospholipid component (ΔCH_2) increases. Interestingly, we found a linear relationship between the Laurdan GP and ΔCH_2. In previous work we concluded that the lines we observed on the DLPC/DPPC GUV surface at temperatures corresponding

to the phase coexistence are composed mainly of DPPC but contain a fraction of DLPC (Bagatolli and Gratton, 2000). Also because of the progressive increment in the solid line domain thickness when the temperature decreases, the fluid DLPC matrix may contain a fraction of DPPC molecules. For the DLPC/DPPC mixture, we postulated that the DLPC molecules that crystallize on the DPPC solid domains can introduce structural defects on the solid domain structures that favor water penetration (Bagatolli and Gratton, 2000). In addition, the fraction of DPPC molecules that remains in the fluid phase should increase the packing of the fluid phase, thus decreasing the effect of the water relaxation process. The main consequence of the last phenomenon is that the difference between the GP values obtained on the solid and fluid domains should be small, as we found in our experiments, showing a strong influence between the fluid and solid phases (Parasassi et al., 1993; Bagatolli and Gratton, 2000). Taking into account the linear relationship between GP and ΔCH_2 for the different mixtures containing DLPC (Fig. 5), we conclude that 1) the fraction of DLPC that cocrystallizes with the second phospholipid component decreases in the following order: DPPC > DSPC > DAPC; 2) the amount of the second phospholipid component in the DLPC fluid matrix decreases as DPPC > DSPC > DAPC. Consequently, for saturated phospholipid binary mixtures containing PC in the polar headgroup, we conclude that at the phase coexistence temperature regime the influence between the fluid and solid phases gradually increases as ΔCH_2 decreases. This conclusion is in agreement with the information contained in the phase diagrams of the phospholipid binary mixtures (Van Dijck et al., 1977; Mabrey and Sturtevant, 1976) and the observations made with computer simulations in PC-containing binary mixtures increasing the hydrophobic mismatch (Jørgensen et al., 1993).

As we pointed out in the Results, based on the Laurdan GP results, the domain coexistence in DLPC/DAPC is between pure fluid and pure gel lipid domains. This last finding is in agreement with those observed in DPPE/DPPC and DMPE/DMPC mixtures. Therefore, we concluded that in the DLPC/DAPC (1:1 mol/mol), DPPE/DPPC (7:3 mol/mol), and DMPE/DMPC (7:3 mol/mol) mixtures the fraction of the low melting temperature phospholipid component (DLPC, DPPC, and DMPC, respectively) in the solid domains (composed of DAPC, DPPE, and DMPE, respectively) is negligible.

In previous work we reported a linear dependence between the Laurdan GP and the intermolecular spacing among the lipid molecules in single-component aggregates formed of different glycosphingolipid (GSLs) and phospholipids (Bagatolli et al., 1998). We explain this observation by considering the model introduced by Parasassi et al., i.e., Laurdan in the lipid aggregates resides in sites containing different amounts of water, and the dimensions of these sites are related to the lipid molecular structure and lipid packing characteristics (Parasassi et al., 1997; Bagatolli et al., 1998). The results obtained for the different DLPC-containing GUVs clearly confirm the model proposed in our previous work (Bagatolli et al., 1998). These results clearly show the high sensitivity of the GP function to the lipid lateral organization.

Solid-phase temperature regime

Unfortunately, we were not able to obtain a picture of the solid state for the different DLPC-containing mixtures for technical reasons (DLPC has a transition temperature below 0°C). However, a very interesting comparison can be made between the DMPC/DSPC (1:1 mol/mol) and DMPE/DMPC (7:3 mol/mol) mixtures at the temperature regime corresponding to the solid phase. In a comparison of the Laurdan GP histograms for the two mixtures, the solid phase resembles the pure gel phase found in pure phospholipid GUVs (Bagatolli and Gratton, 1999). The GP histogram is narrow, indicating the absence of water dipolar relaxation processes in the solid phase, in agreement with previous results (Parasassi et al., 1997; Bagatolli and Gratton, 1999, 2000). Even though no marked differences were found with Laurdan, a different picture was obtained using *N*-Rh-DPPE.

First we want to point out that the fluorescence intensity images obtained for the DMPE/DMPC mixture with *N*-Rh-DPPE are consistent with those obtained for the DPPE/DPPC (7:3 mol/mol) mixture at the solid temperature regime (Bagatolli and Gratton, 2000). For both PE-containing mixtures we observed coexistence of fluorescent and nonfluorescent regions in the GUV surface (see, for example, Fig. 6 *B*). In our previous work we concluded that the DPPE/DPPC mixture is nonideal, showing solid-solid immiscibility (Bagatolli and Gratton, 2000). This observation was in agreement with the information extracted from the DPPE/DPPC phase diagram (Arnold et al., 1981). A different situation is found for DMPC/DSPC. Below the solid-fluid→solid phase transition the nonfluorescent domains already present in the GUV surface gradually vanished, showing a quasihomogeneous GUV surface at low temperatures. As shown in Fig. 6 *A*, we see some small dark areas on the GUV surface at the solid-phase temperature regime. Lipid miscibility at the solid phase temperature regime for the DMPC/DSPC mixture was reported by Mabrey and Sturtevant and Jørgensen et al., using differential scanning calorimetry and computer simulations, respectively (Mabrey and Sturtevant, 1976; Jørgensen et al., 1993). However, this observation is in contrast with neutron scattering and NMR studies of the same mixture, in which a miscibility gap was reported (Sackmann, 1994). Our experiments suggest partial lipid miscibility for the DMPC/DSPC mixtures below the solidus line. Only a few domains remain as the temperature is lowered past the solidus line, and the surface of the vesicles appears to be relatively homogeneous. Given the spatial resolution of our microscope, we

cannot exclude the existence of domains smaller than the pixel size.

We want to remark that at the phase coexistence temperature regime *N*-Rh-DPPE shows a total segregation from the DMPE gel domains, in agreement with observations of DPPE/DPPC mixtures (Bagatolli and Gratton, 2000). *N*-Rh-DPPE possesses a very large polar headgroup because of the rhodamine moiety, and the very stable arrangement of the DMPE and DPPE gel phase (Boggs, 1987) prevents the insertion of this fluorescent probe into the DMPE or DPPE gel phase. At the solid temperature regime *N*-Rh-DPPE in the DMPE/DMPC mixture is forced to stay in the DMPE solid domains because of lipid immiscibility. The same phenomenon was observed in the DPPE/DPPC mixture (Bagatolli and Gratton, 2000). Therefore, at the solid temperature regime, the free diffusion of the *N*-Rh-DPPE on the entire GUV surface requires lipid miscibility, as we observed in DMPC/DSPC mixture.

CONCLUDING REMARKS

Compared with the traditional fluorescence studies involving lipid vesicles, our microscopic experimental approach offers a variety of unique advantages. The combination of the two-photon excitation images, obtained with polarized excitation light, and the fluorescent and partition properties of Laurdan and *N*-Rh-DPPE molecules became an ideal tool for the study of the fluid, fluid-solid, and solid temperature regimes in GUVs composed of different lipid mixtures. Our approach allows direct visualization of the microscopic scenario, providing information of lipid domain shapes and dynamics, with information of the lipid phase state. In the present work we reported the first correlation between lipid domain shape and binary phospholipid mixture composition in unsupported lipid bilayers. We also demonstrated that solid domains spanning the lipid bilayer are a general phenomenon in saturated phospholipid binary mixtures.

We thank Dr. J. D. Müller for the help in the chamber design and for the chamber construction and Dr. D. M. Jameson for critical reading of the manuscript.

This work was supported by National Institutes of Health grant RR03155. LAB is a recipient of a CONICET (Argentina) fellowship.

REFERENCES

Angelova, M. I., and D. S. Dimitrov. 1986. Liposome electroformation. *Faraday Discuss. Chem. Soc.* 81:303–311.

Angelova, M. I., N. Hristova, and I. Tsoneva. 1999. DNA-induced endocytosis upon local microinjection to giant unilamellar cationic vesicles. *Eur. Biophys. J.* 28:142–150.

Angelova, M. I., S. Soléau, Ph. Meléard, J. F. Faucon, and P. Bothorel. 1992. Preparation of giant vesicles by external AC fields. Kinetics and application. *Prog. Colloid Polym. Sci.* 89:127–131.

Arnold, K., A. Lösche, and K. Gawrisch. 1981. ^{31}P-NMR investigations of phase separation in phosphatidylcholine/phosphatidylethanolamine mixtures. *Biochim. Biophys. Acta.* 645:143–148.

Bagatolli, L. A., and E. Gratton. 1999. Two-photon fluorescence microscopy observation of shape changes at the phase transition in phospholipid giant unilamellar vesicles. *Biophys. J.* 77:2090–2101.

Bagatolli, L. A., and E. Gratton. 2000. Two photon fluorescence microscopy of coexisting lipid domains in giant unilamellar vesicles of binary phospholipid mixtures. *Biophys. J.* 78:290–305.

Bagatolli, L. A., E. Gratton, and G. D. Fidelio. 1998. Water dynamics in glycosphingolipids studied by Laurdan fluorescence. *Biophys. J.* 75: 331–341.

Bagatolli, L. A., T. Parasassi, G. D. Fidelio, and E. Gratton. 1999. Effect of temperature and lipid composition on giant unilamellar vesicles (GUVs). A two-photon fluorescence microscopy studies, *Biophys. J.* 76:A57.

Bagatolli, L. A., T. Parasassi, and E. Gratton. 2000. Giant phospholipid vesicles: comparison among the whole sample characteristics using different preparation methods. A two-photon fluorescence microscopy study. *Chem. Phys. Lipids.* 105:135–147.

Blume, A., R. J. Wittebort, S. K. Das Gupta, and R. G. Griffin. 1982. Phase equilibria, molecular conformation, and dynamics in phosphatidylcholine/phosphatidylethanolamine bilayers. *Biochemistry.* 21:6243–6253.

Boggs, J. M. 1987. Lipid intermolecular hydrogen bonding: influence on structural organization and membrane function. *Biochim. Biophys. Acta.* 906:353–404.

Caffrey, M., and F. S. Hing. 1987. A temperature gradient method for lipid phase diagram construction using time-resolved x-ray diffraction. *Biophys. J.* 51:37–46.

Dimitrov, D. S., and M. J. Angelova. 1987. Lipid swelling and liposome formation on solid surfaces in external electric fields. *Prog. Colloid Polym. Sci.* 73:48–56.

Evans, E., and R. Kwok. 1982. Mechanical calorimetry of large dimyristoylphosphatidylcholine vesicles in the phase transition region. *Biochemistry.* 21:4874–4879.

Glaser, M. 1992. Characterization and formation of lipid domains in vesicles and erythrocyte membranes. *Comm. Mol. Cell. Biophys.* 8:37–51.

Gliss, C., H. Clausen-Schaumann, R. Gunther, S. Odenbach, O. Randl, and T. M. Bayerl. 1998. Direct detection of domains in phospholipid bilayers by grazing incidence diffraction of neutrons and atomic force microscopy. *Biophys. J.* 74:2443–2450.

Grainger, D. W., A. Reichert, H. Ringsdorf, and C. Salesse. 1990. Hydrolytic action of phospholipase A2 in monolayers in the phase transition region: direct observation of enzyme domain formation using fluorescence microscopy. *Biochim. Biophys. Acta.* 1023:365–379.

Haverstick, D. M., and M. Glaser. 1987. Visualization of Ca^{2+}-induced phospholipid domains. *Proc. Natl. Acad. Sci. USA.* 84:4475–4479.

Haverstick, D. M., and M. Glaser. 1989. Influence of proteins on the reorganization of phospholipid bilayers into large domains. *Biophys. J.* 55:677–682.

Holopainen, J. M., M. I. Angelova, and P. K. J. Kinnunen. 2000. Vectorial budding of vesicles by asymmetric enzymatic formation of ceramide in giant liposomes. *Biophys. J.* 78:830–838. .

Ipsen, J. H., and O. G. Mouritsen. 1988. Modelling the phase equilibria in two-component membranes of phospholipids with different acyl-chain lengths. *Biochim. Biophys. Acta.* 944:121–134.

Jørgensen, K., and O. G. Mouritsen. 1995. Phase separation dynamics and lateral organization of two-component lipid membranes. *Biophys. J.* 69:942–954.

Jørgensen, K., M. M. Sperotto, O. G. Mouritsen, J. H. Ipsen, and M. J. Zuckermann. 1993. Phase equilibria and local structure in binary lipid bilayers. *Biochim. Biophys. Acta.* 1152:135–145.

Korlach, J., P. Schwille, W. W. Webb, and G. W. Feigenson. 1999. Characterization of lipid bilayer phases by confocal microscopy and fluorescence correlation spectroscopy. *Proc. Natl. Acad. Sci. USA.* 96: 8461–8466.

Lee, A. G. 1975. Fluorescence studies of chlorophyll a incorporated into lipid mixtures, and the interpretation of "phase" diagrams. *Biochim. Biophys. Acta.* 413:11–23.

Lentz, B. R., Y. Barenholtz, and T. E. Thompson. 1976. Fluorescence depolarization studies of phase transitions and fluidity in phospholipid bilayers. 2. Two-component phosphatidylcholine liposomes. *Biochemistry.* 15:4529–4537.

Longo, M. L., A. J. Waring, L. M. Gordon, and D. A. Hammer. 1998. Area expansion and permeation of phospholipid membrane bilayers by influenza fusion peptides an mellitin. *Langmuir.* 14:2385–2395.

Mabrey, S., and J. M. Sturtevant. 1976. Investigation of phase transition of lipids and lipid mixtures by high sensitivity differential scanning calorimetry. *Proc. Natl. Acad. Sci. USA.* 73:3862–3866.

Mathivet, L., S. Cribier, and P. F. Devaux. 1996. Shape change and physical properties of giant phospholipid vesicles prepared in the presence of an AC electric field. *Biophys. J.* 70:1112–1121.

Meléard, P., C. Gerbeaud, P. Bardusco, N. Jeandine, M. D. Mitov, and L. Fernandez-Puente. 1998. Mechanical properties of model membranes studied from shape transformations of giant vesicles. *Biochimie.* 80: 401–413.

Meléard, P., C. Gerbeaud, T. Pott, L. Fernandez-Puente, I. Bivas, M. D. Mitov, J. Dufourcq, and P. Bothorel. 1997. Bending elasticities of model membranes: influences of temperature and sterol content. *Biophys. J.* 72:2616–2629.

Menger, F. M., and J. S. Keiper. 1998. Chemistry and physics of giant vesicles as biomembrane models. *Curr. Opin. Chem. Biol.* 2:726–732.

Merkel, R., E. Sackmann, and E. Evans. 1989. Molecular friction and epitactic coupling between monolayers in supported bilayers. *J. Physique.* 50:1535–1555.

Möhwald, H., A. Dietrich, C. Böhm, G. Brezesindki, and M. Thoma. 1995. Domain formation in monolayers. *Mol. Membr. Biol.* 12:29–38.

Mouritsen, O. G. 1998. Membranes display nano-scale heterogeneity—beating the randomness of the fluid lipid bilayer. *Biol. Skr. Dan. Vid. Selsk.* 49:47–53.

Needham, D., and E. Evans. 1988. Structure and mechanical properties of giant lipid (DMPC) vesicles bilayers from 20°C below to 10°C above the liquid crystal-crystalline phase transition at 24°C. *Biochemistry.* 27: 8261–8269.

Needham, D., T. M. McIntosh, and E. Evans. 1988. Thermomechanical and transition properties of dimyristoylphosphatidylcholine/cholesterol bilayers. *Biochemistry.* 27:4668–4673.

Parasassi, T., G. De Stasio, A. d'Ubaldo, and E. Gratton. 1990. Phase fluctuation in phospholipid membranes revealed by Laurdan fluorescence. *Biophys. J.* 57:1179–1186.

Parasassi, T., G. De Stasio, G. Ravagnan, R. M. Rusch, and E. Gratton. 1991. Quantitation of lipid phases in phospholipid vesicles by the generalized polarization of Laurdan fluorescence. *Biophys. J.* 60: 179–189.

Parasassi, T., and E. Gratton. 1995. Membrane lipid domains and dynamics detected by Laurdan. *J. Fluorescence.* 5:59–70.

Parasassi, T., E. Gratton, W. Yu, P. Wilson. and M. Levi. 1997. Two photon fluorescence microscopy of Laurdan generalized polarization domains in model and natural membranes. *Biophys. J.* 72:2413–2429.

Parasassi, T., E. Krasnowska, L. A. Bagatolli, and E. Gratton. 1998. Laurdan and Prodan as polarity-sensitive fluorescent membrane probes. *J. Fluorescence.* 8:365–373.

Parasassi, T., G. Ravagnan, R. M. Rusch, and E. Gratton. 1993. Modulation and dynamics of phase properties in phospholipid mixtures detected by Laurdan fluorescence. *Photochem. Photobiol.* 57:403–410.

Raudino, A. 1995. Lateral inhomogeneous lipid membranes: theoretical aspects. *Adv. Coll. Interface Sci.* 57:229–285.

Sackmann, E. 1978. Dynamic molecular organization in vesicles and membranes. *Ber. Bunsenges. Phys. Chem.* 82:891–909.

Sackmann, E. 1994. Membrane bending energy concept of vesicle and cell shapes and shape transitions. *FEBS Lett.* 346:3–16.

Sackmann, E., and T. Feder. 1995. Budding, fission and domain formation in mixed lipid vesicles induced by lateral phase separation and macromolecular condensation. *Mol. Membr. Biol.* 12:21–28.

Shimshick, E. J., and H. M. McConnell. 1973. Lateral phase separation in phospholipid membranes. *Biochemistry.* 12:2351–2360.

So, P. T. C., T. French, W. M. Yu, K. M. Berland, C. Y. Dong, and E. Gratton. 1995. Time resolved fluorescence microscopy using two-photon excitation. *Bioimaging.* 3:49–63.

So, P. T. C., T. French, W. M. Yu, K. M. Berland, C. Y. Dong, and E. Gratton. 1996. Two-photon fluorescence microscopy: time-resolved and intensity imaging in fluorescence imaging spectroscopy and microscopy. X. F. Wang and B. Herman, editors. Chemical Analysis Series, Vol. 137. John Wiley and Sons, New York. 351–374.

Van Dijck, P. W. M., A. J. Kaper, H. A. J. Oonk, and J. De Gier. 1977. Miscibility properties of binary phosphatidylcholine mixtures. A calorimetric study. *Biochim. Biophys. Acta.* 470:58–69.

Weis, R. M., and H. M. McConnell. 1985. Cholesterol stabilizes the crystal-liquid interface in phospholipid monolayers. *J. Phys. Chem.* 89:4453–4459.

Wick, R., M. I. Angelova, P. Walde, and P. L. Luisi. 1996. Microinjection into giant vesicles and light microscopy investigation of enzyme-mediated vesicle transformation. *Chem. Biol.* 3:105–111.

Yang, L., and M. Glaser. 1995. Membrane domains containing phosphatidylserine and substrate can be important for the activation of protein kinase C. *Biochemistry.* 34:15000–15006.

Yu, W., P. T. So, T. French, and E. Gratton. 1996. Fluorescence generalized polarization of cell membranes: a two-photon scanning microscopy approach. *Biophys. J.* 70:626–636.